Analysis of the plume diversion in the Hall thruster in the near and far fields

Avi Cohen-Zur[†,‡], Amnon Fruchtman[‡], and Alon Gany[†]
[†] *Faculty of Aerospace Engineering,*
Technion - Israel Institute of Technology, Haifa 32000, Israel
[‡] *Holon Academic Institute of Technology, P.O. Box 305,*
Holon 58102, Israel
(February 3, 2003)

Plume diversion in the Hall thruster is analyzed by deriving and solving envelope equations. The plume diverges as a result of the plasma pressure that is proportional to the electron temperature. Despite the radial plasma expansion, a high heat conductivity makes the decrease of the electron temperature along the flow very slow. As a result, the plume diversion becomes large. The radial magnetic field at the plasma exhaust inhibits a large heat flux. On one hand, the smaller heat conductivity of the magnetized plasma results in a cooling of the electrons as they cross the magnetic field. On the other hand however, the reduced mobility of the magnetized electrons results in an ambipolar electric field that tends to heat the electrons. We show that there is an optimal intensity of the magnetic field, at which the temperature of the electrons that cross the magnetic field is minimal and at which, therefore, the plume diversion is minimal.

I. INTRODUCTION

A crucial issue in the Hall thruster performance is achieving a better plume collimation. Decreasing the plume angle below 90° should reduce the erosion of surfaces, especially the solar panels, by impacting ions. Also, a less divergent plume should result in a smaller interference with the RF transmission that is used for communication. The plume divergence is caused by the nonuniformity of the magnetic field and by the radial force exerted on the plasma by the electron pressure. A considerable theoretical and experimental effort has been made over the past few years in order to understand the evolution of the plume. [1]- [9] Reducing plume diversion by use of segmented electrodes has been recently demonstrated. [10]

The plume diversion is caused mostly by the curvature of the magnetic field lines and by the plasma pressure. At the exhaust, outside the acceleration region, the plasma pressure seems to be the main source of the plume diversion. In this paper we focus on the exhaust region, the region beyond the cathode. We theoretically analyze the plume diversion in the exhaust of the Hall thruster by deriving and solving a derived set of quasi two-dimensional envelope equations. Since the source of the plume diversion is the plasma pressure the extent of the diversion depends on the evolution of the electron temperature. If both magnetic field and heat conductivity are zero the electron temperature decreases adiabatically to zero as the plasma expands and the asymptotic value of the plasma perpendicular velocity can be determined analytically. The large electron heat conductivity makes the decrease of the electron temperature along the flow very slow. As a result, the plume diversion becomes large. The radial magnetic field at the plasma exhaust however, inhibits a large heat flux.

This smaller heat conductivity of the magnetized plasma results in a cooling of the electrons as they cross the magnetic field, reducing the plume diversion. The magnetic field however, also has an opposite effect on the electrons. The reduced mobility of the electrons while they move across the magnetic field results in an ambipolar electric field that tends to heat the electrons. We show that there is an optimal intensity of the magnetic field at which the temperature of the electrons that cross the magnetic field is minimal, and, at which, therefore, the plume diversion is minimal.

II. THE MODEL

We start with the two dimensional, slab geometry, combined electron and ion quasineutral plasma equations. Ions are treated as a cold fluid. Quasineutrality and the fact that in the plume there is no net current yield that the electrons must follow the ions at the same axial and transverse velocity. The axial direction, the direction of the thrust vector, is denoted by z and the plume diverges in the x direction. The azimuthal direction is denoted by the ignorable coordinate y. The slab geometry approximation is fairly good in the near field region, before the annular plasma column expands radially and crosses the axis of symmetry. The model will be modified for cylindrical geometry in later work. A transverse magnetic field B_x is present. The magnetic field intensity varies along the z axis, and we neglect the axial component of the magnetic field. In the present work we use a magnetic profile of the form

$$B_x = B_0 \exp\left[-\frac{(z-z_m)^2}{L_m^2}\right] \ , \tag{1}$$

with z_m a location inside the thruster channel and L_m being the characteristic width. The plasma dynamics is governed by the continuity equation

$$\frac{\partial}{\partial x}(nv_x) + \frac{\partial}{\partial z}(nv_z) = 0, \tag{2}$$

and by the momentum equation

$$\frac{\partial}{\partial x}\left(m_i n v_x^2\right) + \frac{\partial}{\partial z}(m_i n v_z v_x) = -\frac{\partial}{\partial x}(nT_e) \ , \tag{4}$$

$$\frac{\partial}{\partial x}(m_i n v_x v_z) + \frac{\partial}{\partial z}(m_i n v_z^2) = -\frac{\partial}{\partial z}(nT_e) \ - m_e n v_z \frac{\omega_c^2}{\nu}, \tag{5}$$

where n is the particle density, v_x and v_z are the ion and electron equal transverse and axial velocities, m_i and m_e are the ion and electron masses, T_e is the electron temperature, and ν and ω_c are the electron collision and cyclotron frequencies. We assume that the ions are unmagnetized. The combined energy equation for the plasma becomes

$$\frac{\partial}{\partial x}\left\{\left[\frac{m_i}{2}\left(v_x^2+v_z^2\right)+\frac{5}{2}T_e\right]nv_x\right\}+\frac{\partial}{\partial z}\left\{\left[\frac{m_i}{2}\left(v_x^2+v_z^2\right)+\frac{5}{2}T_e\right]nv_z\right\}=-\frac{\partial q_x}{\partial x}-\frac{\partial q_z}{\partial z}\ , \tag{6}$$

where $q_{z,x}$ is the heat flux in the z, x direction.

For the derivation of the envelope equations we integrate the equations in the x direction over the entire plume, thus obtaining equations for the average values of the plasma variables at each axial location. The resulting equations are quasi one-dimensional, while we solve for the transverse diversion of the beam. This formalism turns out to be both simple and powerful in analysing the plume evolution.

The integrated equations are the continuity equation

$$nv_z a=\Gamma_0\ , \tag{7}$$

the x component of the momentum equation

$$m_i\Gamma_0\frac{dv_x}{dz}=nT_e\ , \tag{8}$$

the z component of the momentum equation

$$\frac{d}{dz}\left[a\left(nm_iv_z^2+nT_e\right)\right]=-m_e\Gamma_0\frac{\omega_c^2}{\nu}\ , \tag{9}$$

and the energy equation

$$\Gamma_0\frac{d}{dz}\left[\frac{m_i}{2}\left(v_x^2+v_z^2\right)+\frac{5}{2}T_e\right]=-\frac{d}{dz}\left(aq_z\right)\ , \tag{10}$$

where a measures the plume half width and Γ_0 is the half particle flux of the plume per width unit (in the y direction). To the above equations we add an equation, the "averaged streamline" equation, of the form

$$\frac{da}{dz}=\frac{v_x}{v_z}\ , \tag{11}$$

and an expression for the heat flux

$$q_z=-\kappa\frac{dT_e}{dz}\ , \tag{12}$$

with a heat coefficient κ. In equations (7) through (12) all the variables, such as v_x, v_z, n, and T_e are the averaged variables.

It can be shown that the conversion of the two-dimensional equations into envelope equations is consistent with additional relations between the variables. For example, in the case of no heat conductivity and no magnetic field the flow is adiabatic. In the two dimensional formalism it follows that in this case $T_e n^{\gamma-1}$ is constant along a streamline. In the envelope

equations, for this case, it can be shown that $T_e n^{\gamma-1}$ is constant along the z axis for the averaged values of T_e and n. To do that we write the energy equation in terms of the entropy $s = \ln\left(T_e^{3/2}/n\right)$:

$$\Gamma_0 T_e \frac{ds}{dz} = -\frac{d}{dz}\left(aq_z\right) + m_e \Gamma_0 \frac{\omega_c^2}{\nu} v_z \ . \tag{13}$$

Here the effects of the magnetic field and the heat conductivity on the variation of the entropy as the plume develops are evident. This equation shows clearly that the entropy is constant in the absence of magnetic field and heat conduction.

Equations (7) through (12) are complemented with a set of boundary conditions. We assume that the axial and transverse velocities and the electron temperature are specified at the channel exit plane, which coincides with the cathode/neutralization plane, which we denote as $z = 0$. The value of a at $z = 0$ is taken as the channel half width. Because the derivative of the heat flux in Eq. (10) is proportional to the second derivative of the temperature, two boundary conditions are required for the temperature. In addition to specifying the temperature at the cathode, we require that the temperature be bounded at infinity. Since the transverse velocity cannot increase infinitely, it follows from equation (8) that the temperature must asymptotically decrease to zero. The additional boundary condition is, therefore, that the temperature be zero at infinity. The particle flux Γ_0 and the magnetic field intensity along z are input parameters.

III. SOLUTION OF THE EQUATIONS

When a finite heat conductivity is included in the energy equation (10), the set of equations admit solutions for the temperature that grow exponentially to either plus or minus infinity. However, for each set of the input parameters and initial conditions v_z, v_x, T_e, and a, there exists a value of the initial temperature gradient (dT_e/dz) which yields a solution with $T_e \longrightarrow 0$ as the plume evolves. This solution, that lies on the saparatrix which divides the family of solutions between the solutions with $T_e \longrightarrow +\infty$ and $T_e \longrightarrow -\infty$, is the physical solution. A numerical solution to the governing equations must therefore conduct a search for the unique initial temperature gradient which will result in a solution that lies on the separatrix. In order to solve numerically equations (7) through (11), the integration must be performed in the upstream direction, as downstream integration depicts any numerical noise and picks the exponentially growing solution. [11] Since the values of the plasma parameters are not known at a downstream location, the numerical code must perform an additional search of the desired initial conditions.

The numerical solution is performed as follows. Substituting equation (7) into Eqs. (8) and (9), and replacing the electron temperature as a variable by the square of the ion sound

velocity ($c_s^2 = \frac{5}{3}T_e/m_i$), we obtain the x component

$$\frac{dv_x}{dz} = \frac{3}{5}\frac{c_s^2}{a\,v_z} \ , \tag{14}$$

and the z component

$$\frac{d}{dz}\left(v_z + \frac{3}{5}\frac{c_s^2}{v_z}\right) = -\frac{m_e}{m_i}\nu_d \ , \tag{15}$$

of the momentum equation, where $\nu_d = \omega_c^2/\nu$ is the electron diffusion frequency. The energy equation is written in the form:

$$\frac{d}{dz}\left[\frac{1}{2}\left(v_x^2 + v_z^2\right) + \frac{3}{2}c_s^2 - \frac{3}{5}a\frac{\kappa}{\Gamma_0}\frac{dc_s^2}{dz}\right] = 0 \ , \tag{16}$$

hence

$$\frac{1}{2}\left(v_x^2 + v_z^2\right) + \frac{3}{2}c_s^2 - \frac{3}{5}a\frac{\kappa}{\Gamma_0}\frac{dc_s^2}{dz} = \overline{\beta} \ , \tag{17}$$

or

$$\frac{dc_s^2}{dz} = \frac{5}{3}\frac{1}{a}\frac{\Gamma_0}{\kappa}\left[\frac{1}{2}\left(v_x^2 + v_z^2\right) + \frac{3}{2}c_s^2 - \overline{\beta}\right] \ , \tag{18}$$

with $\overline{\beta}$ constant along the axis and hence is equal, in particular, to the left hand side of Eq. (17) calculated at the channel exit plane (taken as $z = 0$).

Downstream the magnetic field vanishes. Along the region in which the magnetic field is negligible the right hand side (RHS) of the momentum equation in the z direction vanishes and Eq. (15) becomes an algebraic relation:

$$v_z + \frac{3}{5}\frac{c_s^2}{v_z} = \overline{p} \ , \tag{19}$$

with a constant $\overline{p}$, which expresses the pressure balance. This relation is substituted into Eqs. (14) and (18). It is possible now to write equations (11), (14), and (18) with c_s^2 as the independent variable. The resulting equation for v_x turns out to be decoupled from the other equations:

$$\frac{dv_x}{dc_s^2} = \left(\frac{3}{5}\right)^2 \frac{\kappa}{\Gamma_0}\frac{c_s^2}{v_z}\left[\frac{1}{2}\left(v_x^2 + v_z^2\right) + \frac{3}{2}c_s^2 - \overline{\beta}\right]^{-1} \ , \tag{20}$$

with v_z expressed by relation (19). Since at the infinity (where $z \longrightarrow \infty$) c_s^2 and hence dc_s^2/dz vanish, it follows from Eq. (17) that at the infinity v_x is bounded and asymptotically approaches:

$$v_{x,\infty} = \sqrt{2\overline{\beta} - \overline{p}^2} \ , \tag{21}$$

with $\overline{p}$ expressing $v_{z,\infty}$. It is therefore possible to solve equation (20) by integration from $c^2_{s,\infty} = 0$ to a finite value $c^2_{s,1}$. The search for the separatrix solution is transformed to a search for the value of $\overline{\beta}$ for which the integration from the initial point $\left(c^2_{s,\infty}, v_{x,\infty}\right) = \left(0, \sqrt{2\overline{\beta} - \overline{p}^2}\right)$ reaches the values $\left(c^2_{s,1}, v_{x,1}\right)$ specified at the cathode. Since Eq. (20) is decoupled from a and z, its integration is possible without dealing with infinite values (which a and z reach) as $c^2_{s,1} \longrightarrow 0$. The considerations that yielded condition (21) result also in the vanishing of the term in the square brackets in the RHS of Eq. (20). We look for a solution in which $c^2_s = 0$ is a regular singular point of Eq. (20) and the integration away from the singularity is performed after an expansion to a small finite value of c^2_s and a corresponding v_x. After v_x and v_z are calculated as functions of c^2_s, and the correct value of $\overline{\beta}$ for the desired $v_{x,1}$ is found, it is possible to integrate the two remaining equations for a and z, in the downstream direction (from $c^2_{s,1}$).

In the region with finite magnetic field it is possible to solve equations (11), (14), (15), and (18) by a straightforward downstream integration, as the heat coefficient κ across the magnetic field is very small. The solutions of the two regions are then matched at a location just downstream of the magnetic field, by setting $\overline{\beta}$ as the same constant for both regions and matching c^2_s and v_x (v_z is immediately matched, and a and z are solved after the match is found).

IV. RESULTS AND DISCUSSION

Equations (11), (14), (15), and (18) were solved for various values of the input parameters, using the method described in the previous section. Results of the calculations are presented for a Xenon gas and for the thruster dimensions: channel half width $a_0 = 7.5$ mm and a median radius of $r_m = 42.5$ mm. The width in the y direction in the slab geometry approximation is the median circumference. At the cathode the temperature is taken as $T_e = 3$ eV, the transverse velocity as $v_{x,0} = 0$, and $v_{z,0} = v_0$. Here $v_0 = \sqrt{2e\phi_A/m_i}$, with ϕ_A, the applied voltage, taken as $\phi_A = 300$ V. The profile of the magnetic field intensity was taken as in Eq. (1) with $z_m = -30$ mm and $L_m = 20$ mm. The mass flux Γ_0 was calculated for $\dot{m} = 5.32$ mg / s.

The heat conduction coefficient was calculated by:

$$\kappa = 3.16 \frac{n T_e}{m_e} \frac{\nu}{\omega_c^2 + \nu^2} \ , \tag{22}$$

where ν and ω_c are the electron collision and cyclotron frequencies. The electron collision frequency is comprised of electron-ion collisions ν_{e-i} and of anomalous collisions ν_{ano}. We assume that the plasma is nearly fully ionized so that electron-neutral collisions are negligible.

The electron-ion collision frequency was taken as following the classical relation:

$$\nu_{e-i} = 2.91 \times 10^{-6} \ln\Lambda \ n T_e^{-3/2} \ , \tag{23}$$

where $\ln\Lambda$ is the Coulomb logarithm, n is in cm^{-3} and T_e in eV. The anomalous collision frequency was taken as Bohm diffusion $\nu_{ano} = \alpha_B \omega_c$ with a somewhat smaller than the classical value of the Bohm coefficient, $\alpha_B = 1/80$ (as in Refs. [12], [13]). From Eq. (22) it follows that in the region of finite magnetic field $\omega_c >> \nu$, and the resulting heat coefficient is very small. As the magnetic field vanishes κ becomes much larger. Also, in this form the density in the expression for κ is cancelled by the density in the expression for ν_{e-i}. This allows for the solution of Eq. (20) independently from the other equations. In the expression for ν_d in Eq. (15) we used only anomalous collisions as the collision mechanism, neglecting the small diffusion in the zero magnetic field region.

Figure 1 presents the calculation results for a typical case ($B_0 = 200$ G). The parameters are presented in the near field only, even though the calculation spans to temperatures near zero. An important result is the temperature behavior within the magnetic field region (solid line). The temperature increases sharply as the magnetically impeded electrons are forced to cross the magnetic field at the same velocity as do the ions. The increase in temperature is due to the work of the internal electric field between the ions and electrons, hence, the ion kinetic energy (and velocity in the z direction) decreases (figure 1 (c)). As the magnetic field intensity drops, κ is increased, allowing heat to flow downstream. The temperature gradient in that region is proportional to the value of the heat conduction coefficient as the total heat flux is approximately constant (the total energy flux is exactly constant). At some point along the plume the drop in temperature levels to much smaller gradients, this is the result of conducting heat with a much higher heat coefficient value. As the magnetic field vanishes the values of the plasma parameters match the values of the zero magnetic field calculations (dashed line). Since only the near field is presented ($z/a_0 \leq 25$), the asymptotic approach of T_e to 0 and of v_x to $v_{x,\infty}$ is not apparent in Fig. 1.

The magnetic field has two opposing effects on the plume diversion. On one hand, it inhibits heat flux and therefore the temperature drops more in the magnetized region, resulting in a reduced plume diversion. On the other hand, it heats the electrons, which results in an increased plume diversion. The dependence of the plume diversion on the magnetic field intensity turns out to be nonmonotonic, and an optimal magnetic field exists. These effects are shown in Figs. 2 and 3. The existence of an optimal configuration should be explored for improving plume collimation.

The effect of the heat conductivity is demonstrated in Figs. 4 and 5. It is clear in the figures that a large heat conductivity results in a slowly decreasing electron temperature and, as a consequence, in a large plume diversion.

V. SUMMARY

The effects of the magnetic field and heat conductivity on the electron temperature in the plume and therefore on the plume diversion have been unfolded. Other sources of plume diversion, such as magnetic field curvature, will be addressed in a future study.

VI. ACKNOWLEDGEMENTS

The authors are grateful to Prof. N. J. Fisch, Dr. Y. Raitses, Dr. J. Ashkenazy, Prof. A. Gallimore to and G. Makrinich for helpful discussions.

This research has been partially supported by a Grant number 1370 from the Israel Ministry of Science Culture and Sport (through the Israel Space Agency) and by a Grant No. 9800145 from the United States-Israel Binational Science Foundation (BSF), Jerusalem, Israel. The support of the Hellen Asher Foundation for Space Research is greatly appreciated.

---

[1] S. Absalamov, V. Andreev, T. Colbert, M. Day, V. Egorov, R. Gnizdor, H. Kaufman, V. Kim, A. Korakin, K. Kozubsky, S. Kudravzev, U. Lebedev, G. Popov, and V. Zhurin, "Measurement of Plasma Parameters in the Stationary Plasma Thruster (SPT-100) Plume and Its Effects on Spacecraft Components", AIAA Paper No. 92-3156, *28th Joint Propulsion Conference* (American Institute of Aeronautics and Astronautics, Washington, DC, 2001).

[2] R. M. Myers and D. H. Manzella, "Stationary Plasma Thruster Plume Characteristics", IEPC paper No. 93-096, 23^{rd} International Electric Propulsion Conference, Seattle, WA, USA, 1993.

[3] D. Oh and D. Hastings, "Experimental Verification of a PIC-DSMC Model for Hall Thruster Plumes", AIAA Paper No. 96-3196, *32nd Joint Propulsion Conference* (American Institute of Aeronautics and Astronautics, Washington, DC, 2001).

[4] F. Darnon, "The SPT-100 Plasma Plume and its Interaction with a Spacecraft, from Modeling to Ground and Flight Characterization", AIAA Paper No. 96-3196, *32nd Joint Propulsion Conference* (American Institute of Aeronautics and Astronautics, Washington, DC, 2001).

[5] L. B. King, A. D. Gallimore, and C. M. Marrese, J. Propul. Power **14**, 327 (1998); L. B. King and A. D. Gallimore, "Ion energy diagnostics in the plasma exhaust plume of a Hall thruster", L. B. King and A. D. Gallimore, J. Propul. Power **16**, 916 (2000); "Mass spectral measurements in the plume of an SPT-100 Hall thruster", J. Propul. Power **16**, 1086 (2000).

[6] M. Keidar and I. D. Boyd, "Effect of a magnetic field on the plasma plume from Hall thrusters", J. Appl. Phys. **86**, 1 (1999).

[7] I. Katz, G. Jongeward, V. Davis, M. Mandell, I. Mikellides, R. Dresseler, I. Boyd, K. Kannenberg, J. Pollard, and D. King, "A Hall Effect Thruster Plume Model Including large-Angle Elastic scattering", AIAA Paper No. 2001-3355, *37th Joint Propulsion Conference* (American Institute of Aeronautics and Astronautics, Washington, DC, 2001).

[8] J. Ashkenazy and A. Fruchtman, "Plasma plume far field analysis", IEPC 01-260, 27^{th} International Electric Propulsion Conference, Pasadena, CA, USA, 2001.

[9] M. Andrenucci, L. Biagioni, and A. Passaro, "PIC/DSMC Models for Hall Effect Thruster plumes: Present Status and ways Forward", AIAA Paper No. 2002-4254, *38th Joint Propulsion Conference*, Indianapolis, IN (American Institute of Aeronautics and Astronautics, Washington, DC, 2002).

[10] Y. Raitses, L. A. Dorf, A. A. Litvak, and N. J. Fisch, J. Appl. Phys. **88**, 1263 (2000); N. J. Fisch, Y. Raitses, L. A. Dorf, and A. A. Litvak, J. Appl. Phys. **89**, 2040 (2001); Y. Raitses, M. Keidar, D. Staack, and N. J. Fisch, J. Appl. Phys. **92**, 4906 (2002).

[11] A. Fruchtman and H. Weitzner, "Fundamental Ion-Cyclotron Frequency Heating in Tokamaks", Phys. Fluids **29**, 1620 (1986).

[12] E. Ahedo, P. Martinez-Cerezo, and M. Martinez-Sanchez, Phys. Plasmas **8**, 3058 (2001).

[13] A. Cohen-Zur, A. Fruchtman, J. Ashkenazy, and A. Gany, "Analysis of the steady-state axial flow in the Hall thruster", Physics of Plasmas **9**, 4363 (2002).

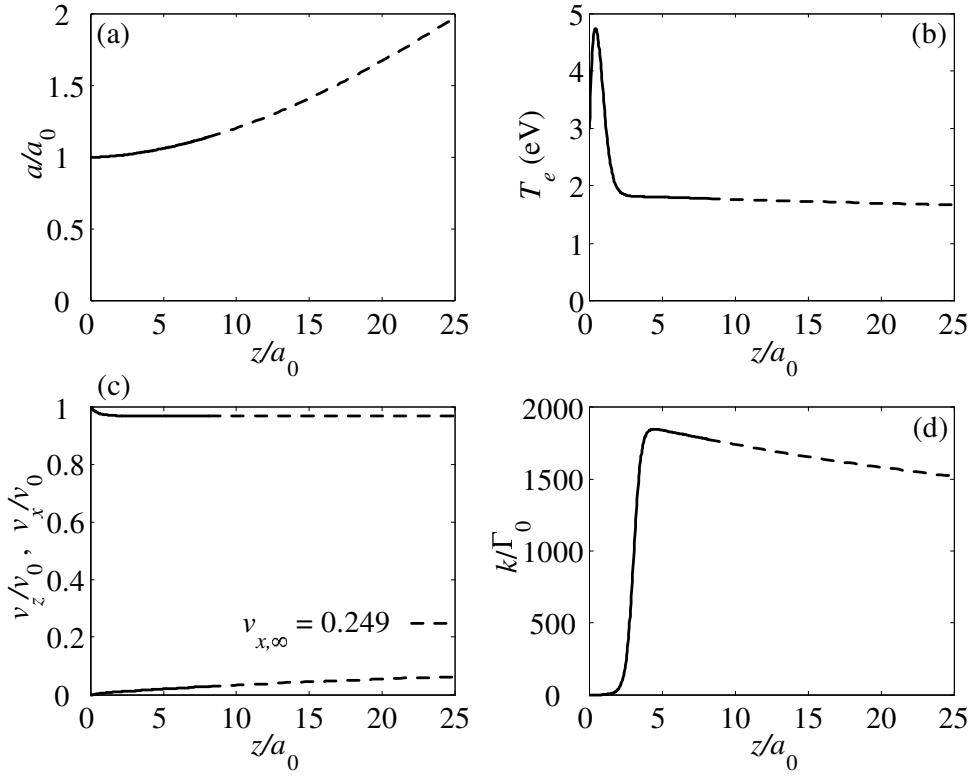

FIG. 1. Typical case near field plasma variables axial profiles. The plume half width (a), electron temperature (b), axial and transverse velocities (c), and the normalized heat coefficient (d). Zero and finite magnetic field regions are denoted by dashed and solid traces respectively. The value of $v_{x,\infty}$ is marked on subplot (c). In this case $B_0 = 200$ G. The input parameter values for this case are: $a_0 = 7.5$ mm, $r_m = 42.5$ mm, $\phi_A = 300$ V, $\dot{m} = 5.32$ mg/s, and $T_e(z = 0) = 3$ eV. The gas is Xenon.

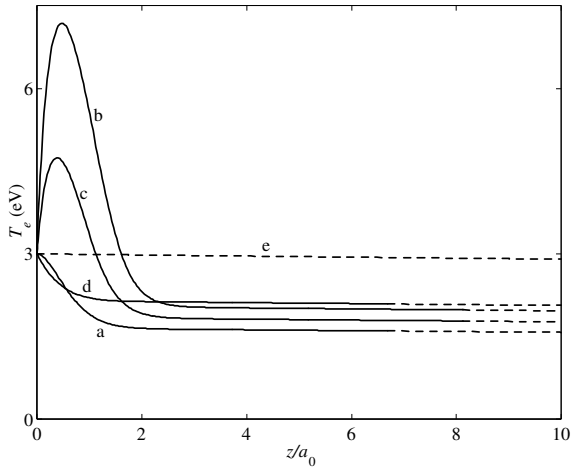

FIG. 2. Axial profile of the electron temperature for various values of B_0. The dashed line represent solution of the unmagnetized region. The traces are: (a) - optimal intensity ($B_0 = 88$ G), (b) - $B_0 = 300$ G, (c) - $B_0 = 200$ G, (d) - $B_0 = 25$ G, (e) - zero magnetic field. The input parameter values are as in Fig. 1.

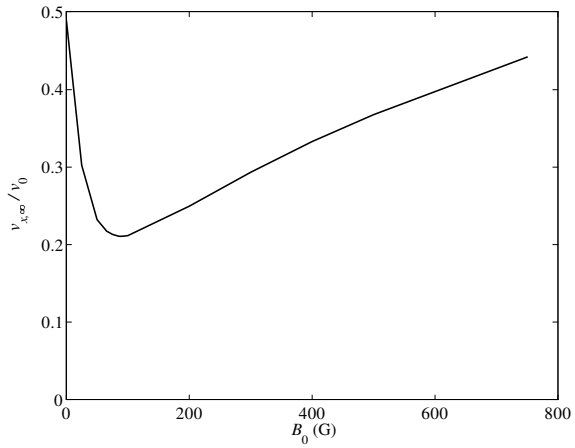

FIG. 3. Dependence of the transverse velocity at infinity on the intensity of the magnetic field. The input parameter values are as in Fig. 1.

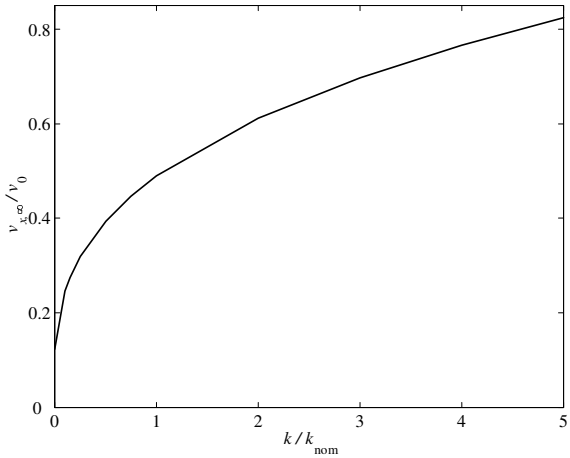

FIG. 4. Dependence of the transverse velocity at infinity on the coefficient of the heat conductivity. The results are for zero magnetic field. The input parameter values are as in Fig. 1.

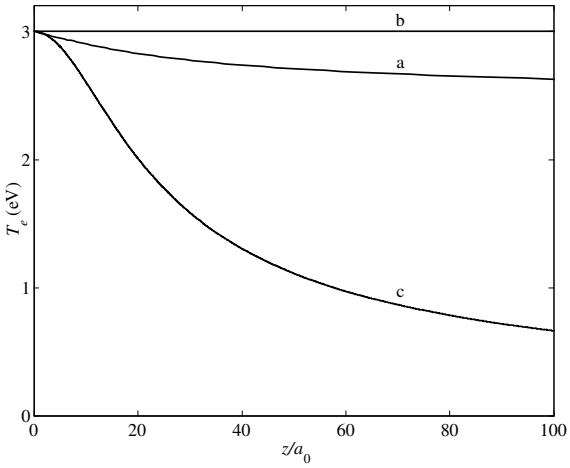

FIG. 5. Axial profile of the electron temperature for various values of the coefficient of heat conductivity. The results are for zero magnetic field and the traces are: (a) - nominal, (b) - infinite conductivity (isothermal case), (c) - zero conductivity (adiabatic case). The input parameter values are as in Fig. 1.